



Contents lists available at [ScienceDirect](https://www.sciencedirect.com)

# Geochimica et Cosmochimica Acta

journal homepage: [www.elsevier.com/locate/gca](http://www.elsevier.com/locate/gca)



## Sources and fate of particulate organic matter along the river-estuary-coastal ocean continuum: Constraints from amino acid and amino sugar carbon isotopes

Jinqiang Guo<sup>a,b</sup>, Eric P. Achterberg<sup>b</sup>, Yuan Shen<sup>c</sup>, Bu Zhou<sup>a,d,e,f</sup>, Jinming Song<sup>a,d,e,f</sup>, Xuegang Li<sup>a,d,e,f</sup>, Liqin Duan<sup>a,d,e,f</sup>, Huamao Yuan<sup>a,d,e,f,\*</sup>

<sup>a</sup> Key Laboratory of Marine Ecology and Environmental Sciences, Institute of Oceanology, Chinese Academy of Sciences, Qingdao 266071, China

<sup>b</sup> Marine Biogeochemistry Division, GEOMAR Helmholtz Centre for Ocean Research Kiel, Kiel 24148, Germany

<sup>c</sup> State Key Laboratory of Marine Environmental Science & College of Ocean and Earth Sciences, Xiamen University, Xiamen 361102, China

<sup>d</sup> Laboratory of Marine Ecology and Environmental Sciences, Qingdao Marine Science and Technology Center, Qingdao 266237, China

<sup>e</sup> University of Chinese Academy of Sciences, Beijing 100049, China

<sup>f</sup> Center for Ocean Mega-Science, Institute of Oceanology, Chinese Academy of Sciences, Qingdao 266071, China

### ARTICLE INFO

Associate editor: Thomas Wagner

#### Keywords:

Compound-specific stable isotopes

Particulate organic matter

Source

Fate

River-estuary-coastal ocean continuum

### ABSTRACT

Estuaries represent hotspots for organic matter cycling. Understanding the sources and fate of organic matter in estuaries is crucial for quantifying the transport of terrestrial organic carbon to the coastal ocean and air-sea carbon dioxide fluxes. Here we report the abundance and carbon isotopic signatures of bulk particulate organic matter (POM) as well as particulate amino sugars and amino acids in surface suspended particles along the salinity gradient in the Changjiang Estuary and adjacent coastal ocean. Our data show that bulk  $\delta^{13}\text{C}$  values are directly related to the  $\delta^{13}\text{C}$  values of essential amino acids, suggesting a control by primary production on bulk  $\delta^{13}\text{C}$  values. A large degree of fractionation ( $-26\%$ ) between phytoplankton  $\delta^{13}\text{C}$  and dissolved inorganic carbon  $\delta^{13}\text{C}$  values was observed in regions with salinities greater than 28, leading to a decline in bulk  $\delta^{13}\text{C}$  values. Examining the  $\delta^{13}\text{C}$  patterns of individual amino sugars and amino acids reveals that terrestrial amino sugars are produced by mixed sources of bacteria, fungi, and algae, while terrestrial amino acids originate from vascular plants and bacteria. Along the salinity gradient, the source of amino sugars shifted to bacteria, whereas amino acids transitioned to algae. Moreover, the low carbon- and nitrogen-normalized yields of amino acids ( $\sim 10\%$  and  $\sim 22\%$ , respectively) observed in the Changjiang River suggest an advanced diagenetic state of terrestrial POM. In contrast, elevated POM reactivity in moderate to high salinity zones indicates contributions from phytoplankton production. Using the bacterial biomarker muramic acid, we found that a substantial portion ( $\sim 19\%$ ) of terrestrial POM is of bacterial origin. Combining the distinct excursions in bulk, amino sugar, and amino acid  $\delta^{13}\text{C}$  values in low salinity ( $< 20$ ) regions of the estuary indicates that terrestrial organic matter is extensively removed in the estuarine regions. Together, these findings underscore significant alterations in the sources and properties of organic matter along the river-estuary-coastal ocean continuum, with bacterial reworking playing an important role.

### 1. Introduction

Estuaries are among the most diverse and dynamic ecosystems, playing a crucial role in the global carbon cycle (Bianchi, 2007; Bianchi et al., 2024). As an interface between land and sea, estuaries receive a significant amount of organic matter from both terrestrial and marine

sources, serving as important regions for organic matter processing (Dagg et al., 2004; Middelburg and Herman, 2007; Canuel and Hardison, 2016). The extent to which organic matter is altered in estuaries determines the transport of organic carbon from land to the coastal oceans and the air-sea carbon dioxide ( $\text{CO}_2$ ) flux. These processes are directly related to the sources and composition of organic matter (Gattuso et al.,

\* Corresponding author at: Key Laboratory of Marine Ecology and Environmental Sciences, Institute of Oceanology, Chinese Academy of Sciences, Qingdao 266071, China.

E-mail address: [yuanhuamao@qdio.ac.cn](mailto:yuanhuamao@qdio.ac.cn) (H. Yuan).

<https://doi.org/10.1016/j.gca.2025.02.004>

Received 3 June 2024; Accepted 3 February 2025

Available online 5 February 2025

0016-7037/© 2025 Elsevier Ltd. All rights are reserved, including those for text and data mining, AI training, and similar technologies.

1998; Cai, 2011). Despite extensive research conducted in estuarine systems over the past few decades, the large variability in the physicochemical environments, coupled with human activities, has led to uncertainties regarding the role of estuaries in the carbon cycle (Cai, 2011; Bauer et al., 2013; Dai et al., 2022). A central challenge in enhancing our comprehension of carbon cycling in estuaries and adjacent coastal areas lies in deciphering the origins and composition of organic matter.

Traditionally, bulk proxies such as the atomic ratio of carbon to nitrogen and also stable carbon isotopes have been used to trace the sources of organic matter (Lamb et al., 2006). These analyses allow for a simple distinction between terrestrial and marine organic matter. However, these bulk parameters provide insufficient specific source information and do not unveil potential variations in composition. Interpretation of bulk  $\delta^{13}\text{C}$  values is not straightforward in estuaries with complex organic matter sources. A major issue arises from the challenge of addressing environmental conditions and the mixing effects of multiple components that contribute to changes in bulk isotope values (Cloern et al., 2002). The bulk  $\delta^{13}\text{C}$  values generally increase along salinity gradients, indicating a contribution from marine phytoplankton (Chanton and Lewis, 1999; Guo et al., 2015). However, several studies have shown that the degree of carbon isotope fractionation between phytoplankton and dissolved inorganic carbon (DIC) is a function of salinity, which may result in decreased bulk  $\delta^{13}\text{C}$  values in high salinity areas (Chanton and Lewis, 1999; Brutemark et al., 2009; Liang et al., 2023).

Biomarkers offer a powerful tool for investigating the sources and cycling of organic matter. A variety of organic molecules such as lignin, fatty acids, and amino acids have been used in studies of estuarine systems (Bianchi and Canuel, 2011; Canuel and Hardison, 2016). Amino acids constitute a major component of living organisms and generally degrade faster than bulk organic matter (Cowie and Hedges, 1994). In the Changjiang Estuary and adjacent areas, Wu et al. (2007) utilized carbon-normalized yields of amino acids and the degradation index (DI) based on amino acid composition to show the elevated reactivity of organic matter in mid-salinity regions. Amino sugars are another less reported yet valuable biomarker, primarily including glucosamine (GlcN), galactosamine (GalN), and muramic acid (MurA). The GlcN/GalN ratio is typically greater than 8 in organic matter enriched in chitin but decreases with ongoing microbial degradation (Müller et al., 1986; Benner and Kaiser, 2003). Relatively low GlcN/GalN values (<3) indicate bacterial sources and diagenetic alteration (Benner and Kaiser, 2003; Davis et al., 2009). In contrast, MurA is exclusively derived from bacteria and allows for tracing the bacterial origin of organic matter (Kaiser and Benner, 2008; Guo et al., 2023b).

Compound-specific isotope analysis (CSIA) provides further insights into the origins of organic matter. The CSIA directly reflects the isotopic signatures of specific molecules, thus facilitating precise identification of both the sources and microbial metabolism associated with organic matter. For instance, the  $\delta^{13}\text{C}$  values of essential amino acids are invariant along the food chain, directly reflecting those of primary producers (Howland et al., 2003; McMahon et al., 2010). Results from Larsen et al. (2013) demonstrate that  $\delta^{13}\text{C}$  patterns of amino acids are a promising tool for unraveling carbon sources in aquatic systems. More recently, Guo et al., (2023a) determined the  $\delta^{13}\text{C}$  values of amino sugars in phytoplankton and heterotrophic bacteria and found that their  $\delta^{13}\text{C}$  patterns have the potential to trace the heterotrophic re-synthesis of organic matter.

Whilst important progress has been made in studying the sources and fate of organic matter in estuaries, many questions remain enigmatic, particularly regarding the rapid loss of terrestrial organic matter signals (Hedges et al., 1997; Canuel and Hardison, 2016; Yin et al., 2023). Previous work suggested that terrestrial organic matter is removed efficiently by biotic (e.g., biodegradation) and abiotic (e.g., flocculation, photodegradation) processes (Dagg et al., 2004; Fichot and Benner, 2014), but other research suggests that it possibly undergoes photo-transformation into unrecognized molecular substances (Stubbins

et al., 2010; Chen et al., 2014). Moreover, along the transition from rivers to the coastal ocean, there is a lack of constraints on the sources of amino acids and amino sugars, changes in organic matter quality (e.g., reactivity), as well as the bacterial origins of organic matter.

The central aim of this study is to investigate the sources and bacterial reworking of particulate organic matter (POM) along the river-estuary-coastal ocean continuum, with the goal of enhancing our understanding of carbon cycling in estuarine systems. Bulk and molecular parameters are employed to characterize POM. We analyzed the concentrations and  $\delta^{13}\text{C}$  values of particulate organic carbon (POC), as well as the abundance and  $\delta^{13}\text{C}$  values of amino sugars and amino acids in surface suspended particles along a salinity gradient from the Changjiang River to the East China Sea. We examined (1) the mechanisms controlling variations in bulk  $\delta^{13}\text{C}$  values, (2) the sources of amino sugars and amino acids, (3) changes in POM reactivity and potential driving factors, and (4) bacterial transformation and bacterial contributions to POM. This study is the first to report carbon isotope values for two classes of amino compounds along the Changjiang Estuary.

## 2. Materials and methods

### 2.1. Sample collection

Sampling was conducted in the Changjiang Estuary and adjacent coastal areas (Fig. 1). The Changjiang River is the third-largest river in the world, with an average annual discharge of  $9.4 \times 10^{11} \text{ m}^3$  over the period from 2012 to 2021 (<https://www.cjh.com.cn/>). Due to the influence of the East Asian monsoon, the majority of the discharge occurs during the wet season (May to October). Large amounts of nutrients and organic matter are transported into the Changjiang Estuary, leading to frequent occurrences of red tides and hypoxia (Zhu et al., 2011; Li et al., 2014). These biological processes, along with hydrodynamics and human activities, contribute to a complex biogeochemical cycle of organic matter in this system.

Suspended particles were sampled along a transect aboard the *R/V Runjiang* in June 2020 (Fig. 1). Surface (0–2 m) water samples were collected using 12-L Niskin bottles, with 1–3 L of seawater immediately filtered onto separate pre-combusted (450 °C, 5h) glass fiber filters (0.7  $\mu\text{m}$ ; Whatman). These filters were stored at  $-20 \text{ }^\circ\text{C}$  until analysis for chlorophyll-a (Chl-a) concentrations, as well as the concentrations and  $\delta^{13}\text{C}$  values of bulk POM, amino sugars, and amino acids. Samples for total suspended matter (TSM) were collected by filtering 1 L of seawater

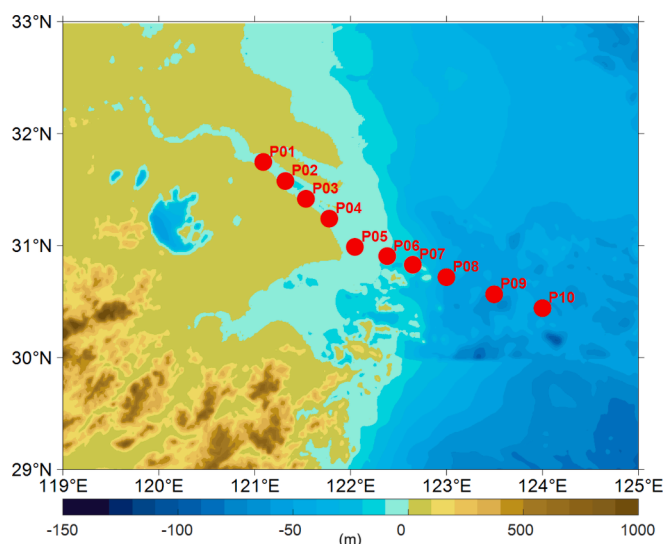


Fig. 1. Sampling stations for suspended particulate matter (SPM) collection (red dots) in the Changjiang Estuary and adjacent coastal areas.

through pre-weighed glass fiber filters (0.7  $\mu\text{m}$ ; Whatman). The filters were then rinsed with deionized water and stored at  $-20\text{ }^{\circ}\text{C}$  before freeze-drying and analysis. At each sampling site, separate filters were used for each analysis to avoid cross-contamination. Temperature and salinity were measured in situ by a conductivity-temperature-depth (CTD) instrument installed on the sampler system.

## 2.2. Measurements of total suspended matter and chlorophyll-a

The content of TSM was determined by weighing the dried particles retained on the filters. Samples for Chl-a analysis were extracted with 10 mL of 90% acetone at  $4\text{ }^{\circ}\text{C}$  for 24h, followed by centrifugation, and subsequent measurement with a fluorescence spectrophotometer (Hitachi F-4600; excitation: 436 nm; emission: 670 nm) (Welschmeyer, 1994). Readings were calibrated using a 7-point calibration curve with a Chl-a standard obtained from Sigma. The detection limit was  $0.1\text{ }\mu\text{g L}^{-1}$ .

## 2.3. Bulk parameter analysis

Samples for bulk characterization were acidified with 1 M hydrochloric acid (HCl) to remove inorganic carbonate, followed by oven-drying at  $60\text{ }^{\circ}\text{C}$  for 24h. The contents of POC and particulate nitrogen (PN), as well as the bulk  $\delta^{13}\text{C}$  values, were analyzed using a Flash IsoLink CN elemental analyzer (EA) coupled with a MAT 253 Plus isotope ratio mass spectrometer (IRMS). Measurements were referenced against international standard reference materials (USGS40, USGS64, and Urea#2a). Stable carbon isotope values were corrected for instrumental drift and reported in units per mil (‰) relative to the Vienna PeeDee Belemnite (VPDB). Analytical precision was 0.02 wt% for carbon content, 0.003 wt% for nitrogen content, and 0.15‰ for bulk  $\delta^{13}\text{C}$  values.

## 2.4. Analysis of amino sugar and amino acid concentrations

The pre-treatment procedure for amino sugar samples followed the methodology reported by Zhu et al. (2014). Particles on glass fiber filters underwent hydrolysis using 6 M HCl at  $105\text{ }^{\circ}\text{C}$  for 8h. Subsequently, the hydrolysates were neutralized to pH  $\sim 6.8$  using 6 M potassium hydroxide and promptly centrifuged. The resultant supernatant was purified using a Supelclean<sup>TM</sup> ENVI-CarbT<sup>TM</sup> Plus solid phase extraction cartridge (400 mg, 1 mL; Sigma-Aldrich) with a recovery rate exceeding 90% to eliminate salts, followed by elution with methanol and dichloromethane. The eluate containing the amino sugars was then concentrated under nitrogen gas and redissolved in deionized water for further instrumental analysis.

Quantification of individual amino sugar concentrations was performed using an ion chromatograph (IC, Dionex ICS-5000<sup>+</sup> SP) coupled with an electrochemical detector. Compound separation was achieved using a PA 20 anion-exchange column ( $3 \times 150\text{ mm}$ ; Thermo Fisher Scientific), preceded by a PA 20 guard column ( $3 \times 30\text{ mm}$ ; Thermo Fisher Scientific). A two-step elution process was employed, with GlcN and GalN eluted with 2 mM sodium hydroxide, while MurA was eluted with 2 mM sodium hydroxide + 200 mM sodium nitrate, at column temperatures of  $25\text{ }^{\circ}\text{C}$  and  $30\text{ }^{\circ}\text{C}$ , respectively (Kaiser and Benner, 2000).

For amino acid analysis, filters were freeze-dried and subsequently hydrolyzed using 6 M HCl at  $110\text{ }^{\circ}\text{C}$  for 24h. The HCl was then removed through repeated drying, and the remaining residue was derivatized using *o*-phthalaldehyde (Lindroth and Mopper, 1979). Separation and detection of amino acids were performed utilizing a Thermo Fisher Scientific U3000 ultrahigh performance liquid chromatography (UPLC) system equipped with a Poroshell 120 EC-C18 column ( $4.6 \times 100\text{ mm}$ ,  $2.7\text{ }\mu\text{m}$  particles) and a fluorescence detector (excitation: 330 nm; emission: 445 nm). The column temperature was maintained at  $30\text{ }^{\circ}\text{C}$ , and the flow rate was set at  $1\text{ mL min}^{-1}$ . A linear binary gradient was employed, commencing with 100% potassium dihydrogen phosphate ( $\text{KH}_2\text{PO}_4$ ;  $48\text{ mmol L}^{-1}$ , pH = 6.25) and transitioning to 61%  $\text{KH}_2\text{PO}_4$  and 39% methanol: acetonitrile (13:1, v/v) at 22 min, 46%  $\text{KH}_2\text{PO}_4$  at

30 min, 40%  $\text{KH}_2\text{PO}_4$  at 37 min, and 20%  $\text{KH}_2\text{PO}_4$  at 39 min (Shen et al., 2017).

## 2.5. Compound-specific $\delta^{13}\text{C}$ analysis of amino sugars and amino acids

Detailed procedures for determining the  $\delta^{13}\text{C}$  values of amino sugars were outlined by Bodé et al. (2009). In brief, following separation via IC (Dionex ICS-5000<sup>+</sup> SP), individual amino sugars were directed into an Isolink interface (Thermo Fisher Scientific) for oxidation to  $\text{CO}_2$ . The oxidizing agent consisted of a mixture of sodium persulfate and phosphoric acid (4%, w/w), flowing at a rate of  $40\text{ }\mu\text{L min}^{-1}$ , with the oxidation reactor maintained at  $99\text{ }^{\circ}\text{C}$ . The resulting  $\text{CO}_2$  was then stripped with helium, dried, and introduced into the IRMS for carbon isotope ratio analysis. An external standard of amino sugars (Sigma-Aldrich) with known  $\delta^{13}\text{C}$  values calibrated by EA-IRMS was prepared to monitor the instrumental analysis. The standard deviations for  $\delta^{13}\text{C}_{\text{GlcN}}$ ,  $\delta^{13}\text{C}_{\text{GalN}}$ , and  $\delta^{13}\text{C}_{\text{MurA}}$  from five injections were  $\pm 0.6\text{‰}$ ,  $\pm 0.6\text{‰}$ , and  $\pm 0.4\text{‰}$ , respectively.

Filters intended for amino acid  $\delta^{13}\text{C}$  values analysis underwent initial freeze-drying, followed by hydrolysis, purification, and derivatization procedures as per previously established protocols (Silfer et al., 1991; McCarthy et al., 2013; McMahan et al., 2018). To ensure accuracy, amino acid reference standards with known  $\delta^{13}\text{C}$  values were injected every three samples to calibrate instrument drift. The determination of amino acid  $\delta^{13}\text{C}$  values was conducted using a Thermo Trace 1310 gas chromatography (GC) coupled with a MAT 253 plus IRMS, employing chromatographic conditions detailed in McMahan et al. (2018). Triplicate injections were performed for each sample, and the resulting amino acid  $\delta^{13}\text{C}$  values were adjusted for the additional derivatizing reagents according to the procedures outlined by Silfer et al. (1991). The error introduced by derivatization was within 0.25‰, and the standard deviation of replicate injections for individual amino acid  $\delta^{13}\text{C}$  values was found to be  $<0.5\text{‰}$ . A comprehensive analysis was conducted on the  $\delta^{13}\text{C}$  values of eleven amino acids, including alanine (Ala), glycine (Gly), threonine (Thr), serine (Ser), valine (Val), leucine (Leu), isoleucine (Ile), proline (Pro), asparagine + aspartic acid (combined as Asx), glutamine + glutamic acid (combined as Glx), and phenylalanine (Phe).

## 2.6. Index calculation

The carbon- and nitrogen-normalized yields of total particulate amino sugars (TPAS) and total particulate amino acids (TPAA) were calculated as the respective proportions of amino sugar and amino acid carbon or nitrogen to total POC and PN. The  $\delta^{13}\text{C}$  values of essential amino acids ( $\delta^{13}\text{C}_{\text{EAA}}$ ) were determined as the mean isotope values of five amino acids: Ile, Leu, Phe, Thr, and Val. Weighted  $\delta^{13}\text{C}$  values for amino sugars ( $\delta^{13}\text{C}_{\text{WAS}}$ ) and amino acids ( $\delta^{13}\text{C}_{\text{WAA}}$ ) were derived by summing the product of the  $\delta^{13}\text{C}$  value for each amino sugar or amino acid and its relative carbon molar concentration (Kang et al., 2021). The index of variation in amino sugar  $\delta^{13}\text{C}$  values ( $V_{\text{AS}}$ ) was determined as follows:

$$V_{\text{AS}} = \left| \delta^{13}\text{C}_{\text{GalN}} - \delta^{13}\text{C}_{\text{GlcN}} \right| - \left| \delta^{13}\text{C}_{\text{MurA}} - \delta^{13}\text{C}_{\text{GlcN}} \right| \quad (1)$$

The DI was calculated based on multivariate analysis of the mole percentage of protein amino acids according to Dauwe et al. (1999):

$$\text{DI} = \sum_i \left[ \frac{\text{var}_i - \text{AVG var}_i}{\text{STD var}_i} \right] \times \text{fac.coef}_i \quad (2)$$

where  $\text{var}_i$  represents the mole percentage of amino acid *i*,  $\text{AVG var}_i$  and  $\text{STD var}_i$  are the mean and standard deviation of the mole percentage of amino acid *i*, respectively, and  $\text{fac.coef}_i$  is the factor coefficient for amino acid *i* in the first axis of the principal component analysis. These parameters were derived from data generated in our study.

The relative contribution of bacterial organic carbon to POC was

estimated following Tremblay and Benner (2006) and Kaiser and Benner (2008):

$$\text{Bacterial POC (\%)} = \frac{\text{MurA}_{\text{sample}}}{\text{MurA}_{\text{bacteria}}} \times 100 \quad (3)$$

where  $\text{MurA}_{\text{sample}}$  and  $\text{MurA}_{\text{bacteria}}$  are the carbon-normalized yields of MurA in suspended POM and bacteria, respectively. Different  $\text{MurA}_{\text{bacteria}}$  values were used given the variations in bacterial assemblages along the salinity gradient (Bourgoin and Tremblay, 2010). The sampling area was divided into three regions based on salinity: Changjiang River (stations P01 to P04), estuary (stations P05 to P08), and coastal ocean (stations P09 and P10). In the Changjiang River, the end-member value of  $\text{MurA}_{\text{bacteria}}$  was  $42.3 \pm 6.9 \text{ nmol mg C}^{-1}$ , calculated from six Gram-negative heterotrophic bacteria sourced from soil and freshwater, along with one Gram-positive heterotrophic bacterium from soil (Kaiser and Benner, 2008; Tremblay and Benner, 2009). In the estuary, the bacterial assemblage consists of two heterotrophic bacteria from freshwater and soil, as well as two natural coastal populations, resulting in a  $\text{MurA}_{\text{bacteria}}$  value of  $21 \text{ nmol mg C}^{-1}$  (Tremblay and Benner, 2006; Kaiser and Benner, 2008). For the coastal ocean, the  $\text{MurA}_{\text{bacteria}}$  value was  $28.1 \pm 7.1 \text{ nmol mg C}^{-1}$ , reflecting a mixture of 20% autotrophic and 80% heterotrophic marine bacteria (Kaiser and Benner, 2008).

### 3. Results

#### 3.1. Hydrological and chemical characteristics of Changjiang Estuary and adjacent area

In our sampling area, salinity gradually increased seaward from 0.14 to 32.81 (Fig. 2a). The TSM concentrations ranged from  $2.0 \text{ mg L}^{-1}$  to

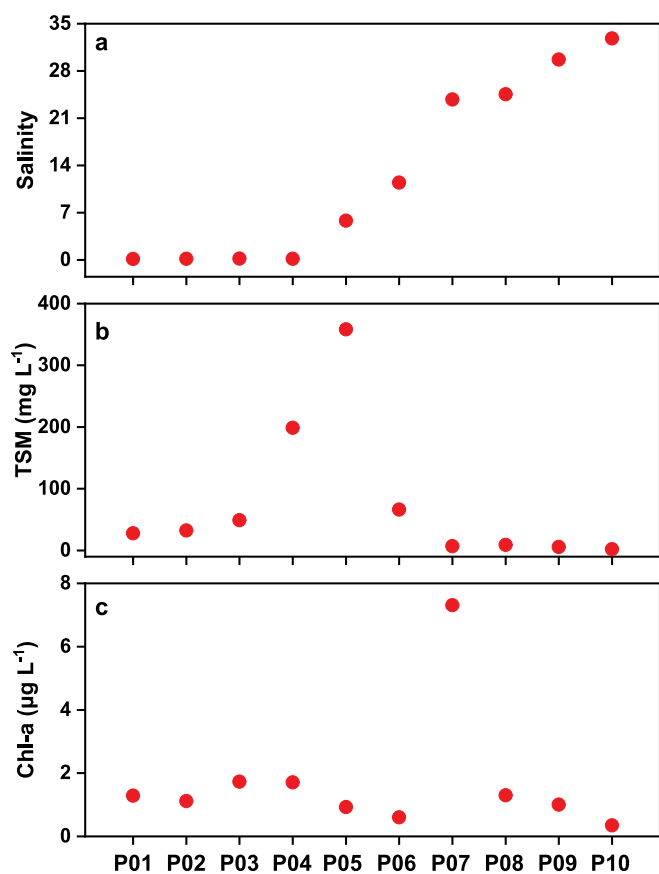


Fig. 2. Distributions of salinity, total suspended matter (TSM) and chlorophyll-a (Chl-a) along the Changjiang River-estuary-coastal ocean continuum. Data points for each site represent a single measurement.

$358.1 \text{ mg L}^{-1}$  (Fig. 2b). Elevated TSM concentrations were observed at stations P04 and P05, suggesting the presence of a turbidity maximum zone at the mouth of the Changjiang River (Jiang et al., 2013). Concentrations of Chl-a were generally low, varying from  $0.3 \text{ µg L}^{-1}$  to  $1.8 \text{ µg L}^{-1}$  along the salinity gradient, except for a peak of  $7.3 \text{ µg L}^{-1}$  observed at station P07 in the moderate salinity ( $\sim 24$ ) zone (Fig. 2c).

#### 3.2. Distributions and properties of POM

The carbon and nitrogen contents of suspended particles varied from 0.6% to 20.8% and 0.1% to 3.1% (normalized to TSM, wt.%), respectively (Fig. 3a, b). Both POC and PN exhibited a similar trend, initially decreasing and then increasing along the salinity gradient. Concentrations of TPAS ranged from  $15.1 \text{ nmol L}^{-1}$  to  $280.3 \text{ nmol L}^{-1}$ . The distributions of TPAS followed a trend similar to TSM and generally decreased with increasing salinity ( $R^2 = 0.50$ ,  $p < 0.05$ ; Fig. 3c). In contrast, TPAA concentrations were considerably variable ( $1.0\text{--}4.2 \text{ µmol L}^{-1}$ ) and did not show a clear pattern with salinity (Fig. 3d).

The ratio of GlcN/GalN in suspended particles varied with a small range from 1.1 to 2.5, without exhibiting a clear trend along the salinity gradient (Fig. 3e). TPAS accounted for 0.2% to 1.7% of POC and 0.4 to 2.2% of PN, with higher TPAS fractions occurring at stations P03 and P04 within the Changjiang River (Fig. 3f). In comparison, TPAA contributed more significantly to POC (7.4–22.5%) and PN (17.7–47.2%). Along the salinity gradient, TPAA (%POC) and TPAA (%PN) exhibited a similar distribution pattern (Fig. 3g, h). Relatively low TPAA (%POC) and TPAA (%PN) values were observed at the river end, with a decreasing trend downstream to station P06. This was followed by a sharp increase at stations P07 and P08, after which a slight decrease towards the stations P09 and P10 (Fig. 3g, h). The highest POC- and PN-normalized yields of amino acids were observed at a salinity of  $\sim 25$ , which is close to the region (salinity:  $\sim 24$ ) with peak Chl-a concentrations.

#### 3.3. Distributions of amino sugar, amino acid and bulk POC $\delta^{13}\text{C}$ values

The  $\delta^{13}\text{C}$  values of three individual amino sugars (GlcN, GalN and MurA) were determined in this study. Values of  $\delta^{13}\text{C}_{\text{GlcN}}$  ( $-50.3\text{‰}$  to  $-18.5\text{‰}$ ) and  $\delta^{13}\text{C}_{\text{MurA}}$  ( $-44.0\text{‰}$  to  $-25.6\text{‰}$ ) showed a similar distribution pattern, first increasing and then decreasing with increasing salinity (Fig. 4a). In contrast, GalN was more enriched in  $^{13}\text{C}$  and exhibited no clear trend in  $\delta^{13}\text{C}$  values (from  $-29.5\text{‰}$  to  $-16.0\text{‰}$ ). Large differences ( $\sim 20\text{‰}$ ) between  $\delta^{13}\text{C}_{\text{GlcN}}$  and  $\delta^{13}\text{C}_{\text{GalN}}$  were observed in the low salinity ( $<7$ ) zone, particularly at the freshwater end, whereas in the middle and high salinity zones, the differences were small ( $\sim 1\text{‰}$ ). Amino acid  $\delta^{13}\text{C}$  values showed a similar pattern along the salinity gradient, gradually increasing from salinity 0.14 to 24.53, then decreasing towards salinity 32.81 (Fig. 4b). Large differences were observed among  $\delta^{13}\text{C}$  values of individual amino acids, with Ser ( $-22.9\text{‰}$  to  $-11.7\text{‰}$ ) being more enriched in  $^{13}\text{C}$  while Glx ( $-38.4\text{‰}$  to  $-30.0\text{‰}$ ) was depleted.

The weighted mean  $\delta^{13}\text{C}$  values of amino sugars and amino acids, as well as  $\delta^{13}\text{C}$  values of essential amino acids were compared with bulk  $\delta^{13}\text{C}$  values. Values of  $\delta^{13}\text{C}_{\text{WAS}}$ ,  $\delta^{13}\text{C}_{\text{WAA}}$ ,  $\delta^{13}\text{C}_{\text{EAA}}$ , and  $\delta^{13}\text{C}_{\text{bulk}}$  varied from  $-39.8\text{‰}$  to  $-18.4\text{‰}$ ,  $-30.7\text{‰}$  to  $-22.4\text{‰}$ ,  $-32.2\text{‰}$  to  $-22.5\text{‰}$ , and  $-28.9\text{‰}$  to  $-21.3\text{‰}$ , respectively (Fig. 5). In general,  $\delta^{13}\text{C}_{\text{WAS}}$ ,  $\delta^{13}\text{C}_{\text{WAA}}$ ,  $\delta^{13}\text{C}_{\text{EAA}}$ , and  $\delta^{13}\text{C}_{\text{bulk}}$  values were distributed in similar patterns over the salinity gradient of 0 to 33. Depleted and relatively constant  $\delta^{13}\text{C}$  values were observed in the Changjiang River. In the estuary, values of  $\delta^{13}\text{C}$  increased with increasing salinity, while the opposite pattern was present in the coastal ocean (Fig. 5). Over the entire salinity interval,  $\delta^{13}\text{C}_{\text{WAA}}$  and  $\delta^{13}\text{C}_{\text{EAA}}$  were closely related to  $\delta^{13}\text{C}_{\text{bulk}}$ , with small offsets occurring in the Changjiang River (1‰ to 4‰). In contrast, the offset between  $\delta^{13}\text{C}_{\text{WAS}}$  and  $\delta^{13}\text{C}_{\text{bulk}}$  was larger ( $\sim 11\text{‰}$ ) in the Changjiang River.

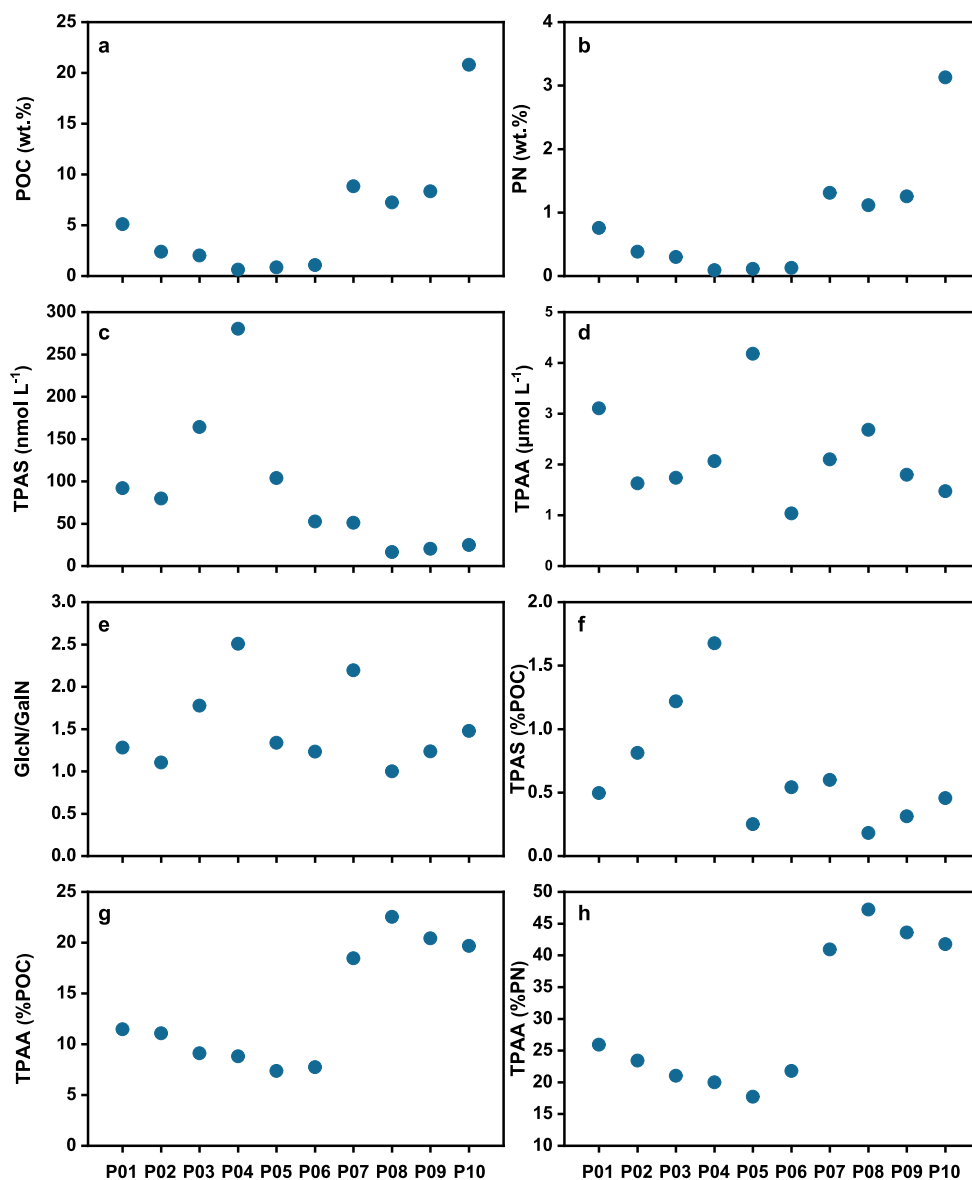


**Fig. 3.** Distributions of (a) particulate organic carbon (POC) content, (b) particulate nitrogen (PN) content, (c) concentrations of total particulate amino sugars (TPAS), (d) concentrations of total particulate amino acids (TPAA), (e) ratio of glucosamine to galactosamine (GlcN/GalN), (f) POC-normalized yields of TPAS, (g) POC-normalized yields of TPAA and (h) PN-normalized yields of TPAA along the Changjiang River-estuary-coastal ocean continuum. Each data point represents one measurement per site.

## 4. Discussion

### 4.1. Mechanisms controlling the variations in bulk $\delta^{13}\text{C}$ values

Large variations in bulk  $\delta^{13}\text{C}$  values ( $\sim 8\%$ ) were observed along the Changjiang River-estuary-coastal ocean continuum (Fig. 5). Biological sources and environmental variables (e.g.,  $\delta^{13}\text{C}_{\text{DIC}}$  and salinity) could contribute to  $\delta^{13}\text{C}_{\text{bulk}}$  excursion. Given that  $\delta^{13}\text{C}_{\text{EAA}}$  directly mirrors the  $\delta^{13}\text{C}$  value of primary producers (Howland et al., 2003; McMahon et al., 2010), the CSIA of amino acids allows us to explicitly distinguish between these intertwined factors. The  $\delta^{13}\text{C}_{\text{bulk}}$  values were significantly correlated with  $\delta^{13}\text{C}_{\text{EAA}}$  ( $R^2 = 0.97$ ,  $p < 0.01$ ), suggesting that POM  $\delta^{13}\text{C}_{\text{bulk}}$  values are largely determined by primary production.

The  $\delta^{13}\text{C}_{\text{bulk}}$  patterns along the salinity gradient are driven by sources of primary producers and associated metabolic fractionation. The  $\delta^{13}\text{C}$  values of terrestrial organic carbon are determined by the relative contributions of C3 and C4 plants. Specifically, the  $\delta^{13}\text{C}$  values of C3 plants typically range from  $-32\%$  to  $-21\%$  (Lamb et al., 2006). In

contrast, due to the more efficient utilization of  $\text{CO}_2$  by the enzyme phosphoenolpyruvate carboxylase, C4 plants exhibit substantially higher  $\delta^{13}\text{C}$  values ( $-13\%$ ) (Lamb et al., 2006). In the Changjiang River, the  $\delta^{13}\text{C}_{\text{bulk}}$  values were notably low, reflecting bulk POC originates from C3 plants. Compared to terrestrial plants, the  $\delta^{13}\text{C}$  values of marine phytoplankton are closely related to  $\delta^{13}\text{C}_{\text{DIC}}$ . The  $\delta^{13}\text{C}_{\text{DIC}}$  values increase progressively with salinity (Wang et al., 2016), and thus in the estuary and adjacent coastal areas,  $\delta^{13}\text{C}$  values of phytoplankton are generally observed to show a pattern similar to that of DIC along the salinity gradient (Chanton and Lewis, 1999; Guo et al., 2015). In our study, the POC  $\delta^{13}\text{C}_{\text{bulk}}$  values in the estuary increased with increasing salinity. However, in the high salinity coastal ocean, the  $\delta^{13}\text{C}_{\text{bulk}}$  values decreased with increasing salinity (Fig. 5). These findings contrast with the trend of a monotone increase in POC  $\delta^{13}\text{C}_{\text{bulk}}$  values with salinity observed in the Pearl River Estuary (Guo et al., 2015). We attribute this to variations in isotopic fractionation between phytoplankton and DIC. In addition to  $\delta^{13}\text{C}_{\text{DIC}}$ , several other factors such as phytoplankton community structure (Hinga et al., 1994), cell size (Popp et al., 1998),

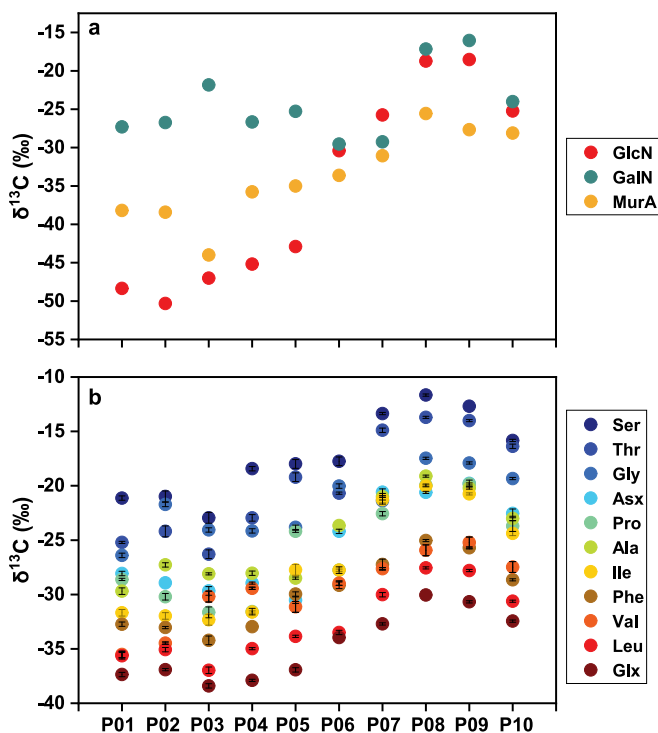


Fig. 4. Variations in  $\delta^{13}\text{C}$  values of amino sugars (a) and amino acids (b) in surface suspended particles along the transect. Error bars represent the standard deviations of triplicate measurements.

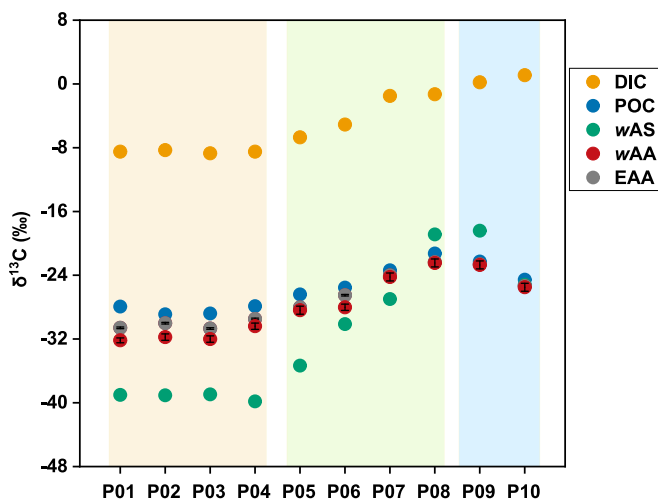


Fig. 5. Variations in the  $\delta^{13}\text{C}$  values of dissolved inorganic carbon (DIC), particulate organic carbon (POC) and essential amino acids (EAA) as well as the weighted mean  $\delta^{13}\text{C}$  values of amino sugars (wAS) and amino acids (wAA) along the transect. The  $\delta^{13}\text{C}$  values of EAA refer to the simple average  $\delta^{13}\text{C}$  values of the five amino acids (isoleucine, leucine, phenylalanine, threonine, and valine).  $\delta^{13}\text{C}$  values of DIC are derived from Wang et al. (2016). Shade with different colors represents Changjiang River (P01 to P04), estuary (P05 to P08), and coastal ocean (P09 and P10) regions, respectively. Error bars represent propagated standard deviations.

growth rate (Burkhardt et al., 1999), salinity (Leboulanger et al., 1995), nutrients (Brutemark et al., 2009), etc., have been shown to influence phytoplankton  $\delta^{13}\text{C}$  signals. Chanton and Lewis (1999) found that the offset between  $\delta^{13}\text{C}_{\text{DIC}}$  and POC  $\delta^{13}\text{C}_{\text{bulk}}$  values in the Apalachicola Bay was roughly  $-20\text{‰}$ . They suggested that this offset varies with salinity, with larger offsets observed in high salinity areas. Similarly, Brutemark

et al. (2009) showed that an increase in salinity leads to a reduction in  $\delta^{13}\text{C}$  values of phytoplankton based on culture experiments. Our results are consistent with these findings. In the estuary, the offset between POC  $\delta^{13}\text{C}_{\text{bulk}}$  and  $\delta^{13}\text{C}_{\text{DIC}}$  values was about  $-20\text{‰}$ , but reached  $-26\text{‰}$  in the high salinity coastal ocean. Shifts in the phytoplankton community might also underlie the decline in POC  $\delta^{13}\text{C}_{\text{bulk}}$  values in the high salinity region. Along the salinity gradient of the Changjiang Estuary, dramatic shifts in phytoplankton community composition have been observed (Jiang et al., 2022). In high salinity zones, cyanobacteria and cryptophytes are typically dominant (Jiang et al., 2015). However, results from laboratory culture experiments indicate that the carbon isotopic signatures of cyanobacteria ( $-33.1\text{‰}$  to  $-8.0\text{‰}$ ) and cryptophytes ( $-20.8\text{‰}$  to  $-8.7\text{‰}$ ) vary widely depending on culture conditions (Popp et al., 1998; Erez et al., 1998; Brutemark et al., 2009). Additionally, Brutemark et al. (2009) suggested that nitrogen limitation leads to a negative deviation in  $\delta^{13}\text{C}$  values of phytoplankton. At stations P09 and P10, the surface concentrations of nitrate were  $2.99 \mu\text{mol L}^{-1}$  and  $0.29 \mu\text{mol L}^{-1}$ , respectively (Guo et al., 2021a). Low concentrations of nitrate are possibly an important factor contributing to the depletion of POC  $\delta^{13}\text{C}_{\text{bulk}}$  values. It is currently unclear whether changes in phytoplankton community composition, salinity, or nutrients dominated the increased offset between  $\delta^{13}\text{C}_{\text{bulk}}$  and  $\delta^{13}\text{C}_{\text{DIC}}$  values in high salinity areas, necessitating further studies for verification.

Abiotic processes (e.g., photo-oxidation) were suggested to possibly alter  $\delta^{13}\text{C}_{\text{bulk}}$  values of terrestrial organic matter (Opsahl and Zepp, 2001). In low salinity areas, particularly at the freshwater end, the  $\delta^{13}\text{C}_{\text{bulk}}$  values of POC were consistently higher than the  $\delta^{13}\text{C}_{\text{EAA}}$  values (Fig. 5). Photo-oxidation of aromatic components in terrestrial organic matter represents a possible explanation for this difference. Terrestrial organic matter is rich in aromatic components such as lignin, which are susceptible to photochemical alteration (Opsahl and Benner, 1998; Feng et al., 2011). Lignin is characterized by depleted  $\delta^{13}\text{C}$  values (by 2–6‰) relative to whole plant material (Benner et al., 1987). The photo-degradation of lignin has been reported to increase the  $\delta^{13}\text{C}_{\text{bulk}}$  values of terrestrial organic carbon (Opsahl and Zepp, 2001). Higher  $\delta^{13}\text{C}_{\text{bulk}}$  values relative to  $\delta^{13}\text{C}_{\text{EAA}}$  in the Changjiang River also appear to be associated with human activities. A study by Wu et al., (2007) in the Changjiang River basin found that POM influenced by anthropogenic activities (e.g., industrial discharges and domestic sewage) exhibits comparably high  $\delta^{13}\text{C}$  values ( $-23\text{‰}$ ). These observations suggest that abiotic processes and anthropogenic perturbations may undermine the reliability of bulk  $\delta^{13}\text{C}$  values in source tracing.

#### 4.2. Constraints on amino sugars and amino acid sources from compound-specific $\delta^{13}\text{C}$ values

Amino sugars and amino acids are important components of POM, constituting approximately 15% of POC (Fig. 3f, g). Particularly in areas with salinity  $>25$ , their contribution to POC exceeded 20% (Fig. 3f, g). However, our current understanding of the sources of amino sugars and amino acids in estuarine regions remains very limited. An important barrier is that the sources of these compounds are diverse (including phytoplankton, zooplankton, bacteria, etc.) and have overlapping or similar compositions. Recent studies indicated that producers of these molecules exhibit distinct amino acid and amino sugar isotopic fingerprints, offering a novel approach to unraveling the multiple sources (Larsen et al., 2013; Guo et al., 2023a).

##### 4.2.1. Sources of amino sugars

Unlike amino acids, which are not effective source markers when D and L enantiomers are not separated, the composition of amino sugars to some extent provides information about their sources. In particular, MurA is considered to originate solely from bacterial cell wall peptidoglycan (Kaiser and Benner, 2008). Identification of the sources of GlcN and GalN relies largely on their ratios. A GlcN/GalN ratio of less than 3 is generally considered to reflect a bacterial origin, while a ratio greater

than 8 indicates a zooplankton signal (Davis et al., 2009; Lehmann et al., 2020). In our study, the GlcN/GalN ratios in surface POM were consistently less than 3 along the salinity gradient, reflecting a bacterial-dominated source of amino sugars. Despite the important role of GlcN/GalN ratio in tracing the origin of amino sugars and the diagenetic alteration of organic matter, there remain several uncertainties related to GlcN/GalN. Primary among these is that the GlcN/GalN value is highly variable across organisms. The GlcN/GalN values in heterotrophic bacteria, photoautotrophic bacteria, copepods, and phytoplankton range from 1.6–3.4, 8.0–56.6, 14.2–20.9, and 0.4–20.5, respectively (Benner and Kaiser, 2003). In particular, the GlcN/GalN ratio of the dinoflagellate *Heterocapsa niei* (0.4) is much lower than that of the diatom *Thalassiosira oceanica* (20.5). In our sampling area, dinoflagellates are an important component of the phytoplankton community (Jiang et al., 2015). The observed lower GlcN/GalN values perhaps imply the contribution of dinoflagellates. Additionally, the GlcN/GalN ratio is significantly affected by microbial degradation (Lehmann et al., 2020; Guo et al., 2023a). Incubation experiments with plankton organic matter showed that the GlcN/GalN ratio rapidly decreased from over 12 to below 3 within three days (Guo et al., 2023a). Overall, these factors raise complexity to the interpretation of GlcN/GalN variations.

Compound-specific  $\delta^{13}\text{C}$  values provide a powerful new set of tracers, allowing differentiation of amino sugar sources between phytoplankton and heterotrophic bacteria. Guo et al. (2023a) performed culture experiments and found distinct  $\delta^{13}\text{C}$  patterns of amino sugars between heterotrophic bacteria and phytoplankton. In phytoplankton, the offset between  $\delta^{13}\text{C}_{\text{GlcN}}$  and  $\delta^{13}\text{C}_{\text{GalN}}$  values was large (4.3–16.6‰), whereas it was small (0.4–4.0‰) in heterotrophic bacteria. We found that in the Changjiang River, the difference between  $\delta^{13}\text{C}_{\text{GlcN}}$  and  $\delta^{13}\text{C}_{\text{GalN}}$  values was much greater than in the estuary and coastal ocean (Fig. 4a). This suggests that amino sugars in estuarine and coastal areas are mainly derived from bacteria. However, inferences regarding phytoplankton-derived amino sugars in the Changjiang River need to be treated with caution. In terrestrial soil organic matter, fungi also contribute significantly to amino sugar abundance (Joergensen, 2018). To date, the  $\delta^{13}\text{C}$  patterns of fungal amino sugars remain unknown. Previous work has shown that fungi are rich in GlcN (Parsons, 2021). If fungi dominate the sources of amino sugars in terrestrial POM, higher GlcN/GalN values would be expected, but this is inconsistent with the

low GlcN/GalN values ( $\sim 1.7$ ) in the Changjiang River. This suggests that terrestrial amino sugars originate from various sources including algae, fungi, and bacteria.

#### 4.2.2. Sources of amino acids

The relative abundance of amino acids is fairly consistent across organisms, limiting the use of individual amino acids as source tracers. Although D-amino acids are considered to be primarily derived from bacteria (Kaiser and Benner, 2008), constraining the sources of the ubiquitous L-amino acids remains challenging.

The  $\delta^{13}\text{C}$  patterns of amino acids provide valuable information for tracing their sources. By analyzing a large number of  $\delta^{13}\text{C}$  values of amino acids from different organisms (bacteria, terrestrial plants, algae, etc.), Larsen et al. (2013) found that the patterns of essential amino acids could serve as isotopic fingerprints to diagnose amino acid producers and are unaffected by changes in environmental conditions. Based on five essential amino acids (Ile, Leu, Phe, Thr, Val), and integrating reported amino acid  $\delta^{13}\text{C}$  data in bacteria, microalgae, seagrasses, and terrestrial vascular plants, we performed linear discriminant analysis. The results showed variations in the origins of amino acids across different salinity zones (Fig. 6). In the freshwater end, amino acids were mainly derived from bacteria and vascular plants. As salinity increased, the sources of amino acids in the estuary gradually shifted to seagrasses and microalgae. In the high salinity coastal ocean, microalgae dominated amino acid production. We noted that the amino acid  $\delta^{13}\text{C}$  signals of seagrasses and microalgae partially overlapped, potentially biasing the identification of amino acid sources in the estuarine area. Previous studies have shown that seagrasses contribute insignificantly to the organic matter in the Changjiang Estuary (Xing et al., 2011; Yao et al., 2015), suggesting that amino acids in the estuarine region mainly originate from microalgae. Overall, we have revealed for the first time changes in the sources of amino acids along the salinity gradient in the Changjiang Estuary on the basis of amino acid  $\delta^{13}\text{C}$  values. These CSIA data demonstrate the complexity of amino acid production in the estuarine and coastal areas, which is not reflected in amino acid concentration and composition.

#### 4.3. Reactivity of POM along the salinity gradient

The fate of POM in estuarine areas is closely linked to its reactivity

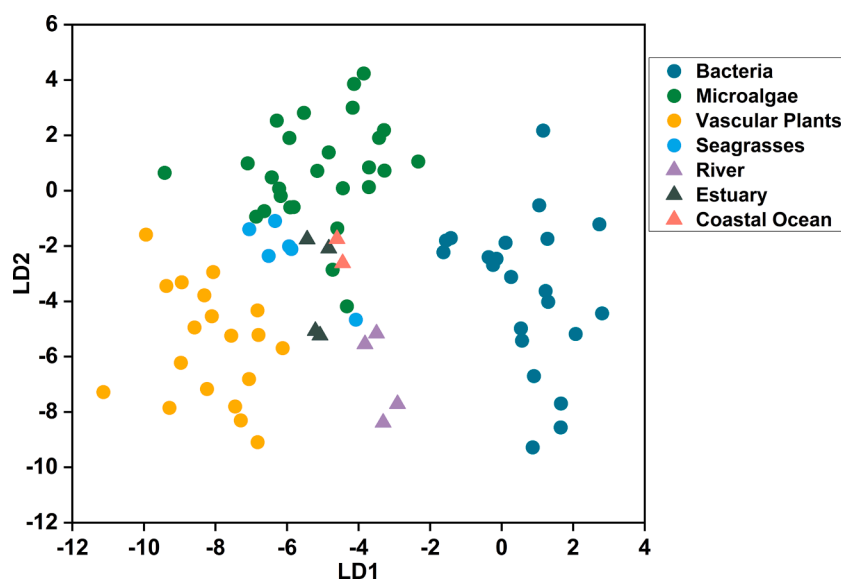


Fig. 6. Linear discriminant function analysis based on the essential amino acid (isoleucine, leucine, phenylalanine, threonine, valine)  $\delta^{13}\text{C}$  values of bacteria, algae, seagrasses and terrestrial plants. River represents samples from stations P01 to P04; Estuary: P05 to P08; Coastal Ocean: P09 to P10. The amino acid  $\delta^{13}\text{C}$  data of bacteria, microalgae, vascular plants, and seagrasses are from Larsen et al. (2013). The  $\delta^{13}\text{C}$  data for lysine were excluded from the linear discriminant analysis due to being below the detection limit.

(Blair and Aller, 2012; Canuel and Hardison, 2016). Amino acids are labile components of POM and are preferentially removed during microbial degradation. A suite of indicators based on amino acid abundance (e.g., carbon- and nitrogen-normalized yields) and composition (e.g., DI and mol% Gly) have been proposed and widely used to assess the diagenetic state of organic matter in marine ecosystems (Cowie and Hedges, 1994; Dauwe et al., 1999; Davis et al., 2009; Lehmann et al., 2020). As diagenesis progresses, amino acid yields and DI values decrease, while the mole percentage of Gly increases. However, it is essential to acknowledge that no single degradation indicator can fully represent the full continuum of organic matter diagenesis. Davis et al. (2009) suggested that the carbon-normalized yield of amino acids is sensitive during early degradation, while DI and molar composition of non-protein amino acids are effective indicators in mid- and late-stage diagenesis, respectively. In this study, multiple degradation indices (e.g., amino acid yields, DI, and mol% Gly) were employed to evaluate the diagenetic state of POM.

A comparison of TPAA (%POC), TPAA (%PN), DI, and mol% Gly (Fig. 3g, h and Fig. 7) indicates that POM in the Changjiang River has undergone extensive diagenetic alteration. This finding aligns with previous studies that suggest a substantial contribution of highly degraded soil organic matter to terrestrial organic matter (Dagg et al., 2004; Wu et al., 2007). Extremely low TPAA (%POC) and TPAA (%PN) values (7.4–7.7% and 17.7–21.8%, respectively) were recorded at stations P05 and P06 in low salinity areas (Fig. 3g, h). These stations are located within the estuarine turbidity zone. Despite sufficient nutrient availability in this region, the high turbidity and hence light limitation impedes phytoplankton photosynthesis. Additionally, resuspension of

refractory sedimentary organic matter further dilutes the amino acid yields in POM.

In contrast, elevated amino acid yields and DI values, along with lower mol% of Gly, were observed in regions with moderate to high salinity (24 to 33). These results suggest that POM in these regions is less altered. The areas where TPAA (%POC) and TPAA (%PN) values were highest showed similar salinities to those with the highest Chl-a concentrations (Fig. 2c and Fig. 3g, h). Similar results were reported by Liang et al. (2023), who found high TPAA yields and Chl-a levels in regions with comparable salinity. Elevated phytoplankton production in moderate salinity zones has been documented in many estuaries and is attributed to a balance of turbidity and nutrient availability (Dagg et al., 2004). In the Changjiang Estuary and adjacent sea, remarkably high Chl-a concentrations and phytoplankton abundance typically occur in regions with salinities between 25 and 31 (Jiang et al., 2015; Guo et al., 2021a). Likewise, Wang et al. (2019) found frequent algal blooms at the front of the Changjiang River plume (salinity ~30). Our results are consistent, highlighting the contribution of phytoplankton production to fresh POM in moderate to high salinity zones.

However, a decline in TPAA (%POC) from 22.5% to 19.6% and TPAA (%PN) from 47.2% to 41.8% was observed from station P08 to station P10, which is inconsistent with the changes in DI and mol% Gly (Fig. 7). The residence time of POM in the water column of the Changjiang Estuary ranged from a few days to a few weeks (Zhu et al., 2006). This suggests that more effective indicators during the early diagenetic stages, such as TPAA (%POC) and TPAA (%PN), reflect a more advanced diagenetic state of POM towards the open ocean. The decline of TPAA (%POC) and TPAA (%PN) is likely driven by decreased nutrient availability in high salinity regions, thereby limiting phytoplankton production. Collectively, our findings provide valuable insights into the reactivity of POM in estuarine environments, underscoring the complex interplay between terrestrial inputs, environmental conditions, and primary production governing the quality of organic matter.

#### 4.4. Transformation and fate of POM along the river-estuary-coastal ocean continuum

Estuaries serve as hotspots for elemental biogeochemical cycling. Unlike the open ocean, which acts as a carbon sink for atmospheric CO<sub>2</sub>, estuaries are typically net heterotrophic and sources of atmospheric CO<sub>2</sub> (Cai, 2011; Dai et al., 2013). Survey results of the air-sea CO<sub>2</sub> flux in the Changjiang Estuary showed an annual release of  $2.5\text{--}5.5 \times 10^{10}$  mol of CO<sub>2</sub> into the atmosphere (Zhai et al., 2007), suggesting significant processing of organic matter in the estuarine region. Several features contribute to the effective role of estuaries as organic matter processors, including (a) high primary productivity, providing labile organic matter as fuel for heterotrophic activity (Cloern et al., 2014); (b) shallow water depth allowing light penetration and promoting photochemical degradation of organic matter (McCallister et al., 2005); (c) tight hydrological interactions between the estuarine and offshore environments, enhancing material exchange (Bianchi, 2007; Snedden et al., 2013).

Global rivers transport ~0.40 Pg of organic carbon to the ocean annually, yet detectable signals of terrestrial organic matter are limited in the open ocean (Hedges et al., 1997). Our bulk and compound-specific  $\delta^{13}\text{C}$  data provide additional evidence to support this conclusion. Particularly in low salinity zones, there is an obvious shift in the  $\delta^{13}\text{C}$  signal, indicating rapid removal of terrestrial organic matter. The mechanisms behind the loss of terrestrial organic matter remain elusive, but some biotic (e.g., biodegradation) and abiotic (e.g., photodegradation and flocculation) processes are considered to contribute to this phenomenon (Bianchi, 2007; Helms et al., 2013; Fichot and Benner, 2014). As discussed in section 4.1, terrestrial organic matter is enriched with aromatic substances such as lignin and tannic acid, which are prone to photodegradation but resistant to microbial utilization (Benner and Kaiser, 2011). Our results, in conjunction with other studies (Dagg et al., 2004; Wu et al., 2007; Liang et al., 2023), also indicate the relatively low

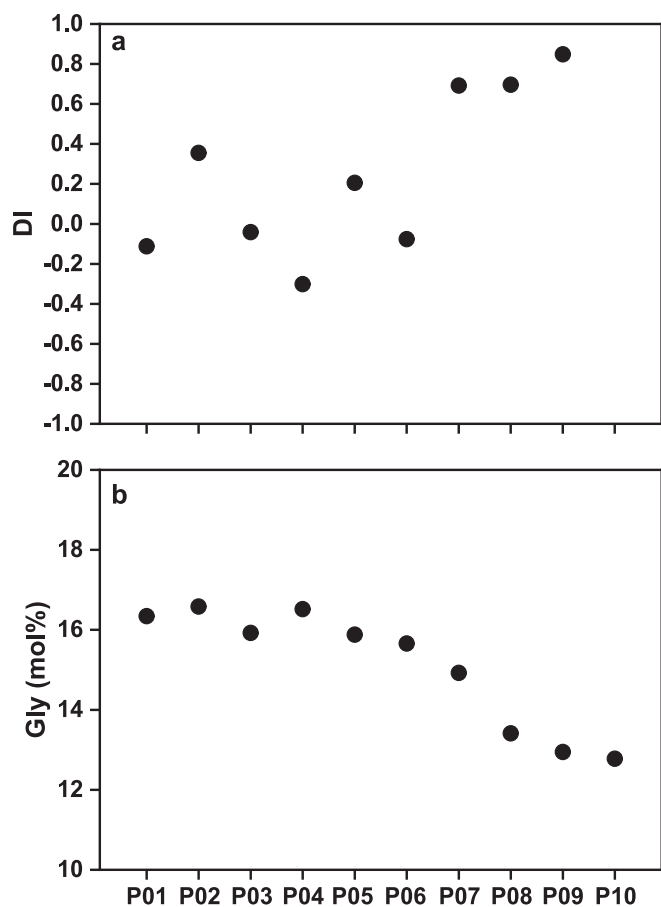


Fig. 7. Changes of degradation index (DI) and mole percentage of glycine (Gly) along the Changjiang River-estuary-coastal ocean continuum. The DI values are derived from a principal component analysis of the mole percentages of protein amino acids (Dauwe et al., 1999).

potential of terrestrial organic matter for microbial degradation. The removal of terrestrial organic matter appears to be attributed to abiotic processes. However, the presence of the turbidity maximum zone in the low salinity area of the Changjiang Estuary partially inhibits radiation penetration (Jiang et al., 2013). Investigations into the annual mineralization of terrestrial dissolved organic carbon (DOC) showed that direct photo-mineralization accounts for a small fraction (6%) (Fichot and Benner, 2014). Additionally, the appreciable discrepancy between the  $\delta^{13}\text{C}$  values ( $-23\text{‰}$  to  $-21\text{‰}$ ) of sedimentary organic carbon (Guo et al., 2021b) and the observed bulk  $\delta^{13}\text{C}$  values of POC ( $-28.9\text{‰}$  to  $-21.3\text{‰}$ ) in the study area suggests that the loss of terrestrial POM signal is unlikely from rapid sinking and burial into sediments. Recent studies have shown that the efficient removal of terrestrial organic matter is largely attributable to the priming effect (Bianchi, 2011; Bianchi et al., 2015; Sanches et al., 2021; Yao et al., 2025). Recognition of the priming effect in estuaries initially centered on fresh organic matter produced by marine phytoplankton promoting the breakdown of refractory terrestrial organic matter. Subsequently, the intrusion of ocean currents is also considered to be an important factor triggering the priming effect (Xu et al., 2018). In the Changjiang Estuary, the invasion of the Kuroshio Current and the Taiwan Warm Current likely enhanced heterotrophic metabolism. Further, photo-transformation might also enhance microbial processing of organic matter. For instance, Fichot and Benner (2014) revealed that approximately 32% of terrestrial DOC is removed on the Louisiana Shelf mixed layer through photo-enhanced biomineralization.

Contrary to the aforementioned perspectives, studies have proposed that terrestrial organic matter could be transformed into undetected components, thereby overestimating the removal of terrestrial organic matter (Stubbins et al., 2010; Chen et al., 2014; Waggoner et al., 2015; Waggoner and Hatcher, 2017). They argue that the photochemical transformation of lignin in terrestrial organic matter results in an increase in bulk  $\delta^{13}\text{C}$  values (Opsahl and Zepp, 2001) and an underestimation of terrestrial organic carbon based on lignin and bulk  $\delta^{13}\text{C}$  estimates. While differences in  $\delta^{13}\text{C}$  values between bulk POC and primary production have been observed in low salinity areas (Fig. 5), the small offset ( $\sim 1.6\text{‰}$ ) is insufficient to support the significant transformation of terrestrial organic matter. Our amino acid and amino sugar  $\delta^{13}\text{C}$  data clearly show changes in their sources in the estuarine area. In particular, the  $\delta^{13}\text{C}$  values of the bacterial biomarker MurA are linked to substrate, with their variations directly reflecting shifts in carbon sources. Furthermore, terrestrial organic matter after photo-transformation is also likely to be consumed by microorganisms (Yin et al., 2023). These findings suggest that the loss of terrestrial organic matter signal in the ocean is unlikely due to extensive transformation into undetectable substances.

In aquatic settings, heterotrophic bacteria serve as primary agents of organic matter decomposition and diagenetic alteration. The above discussion highlights the significant role of bacteria in the removal of terrestrial organic matter. However, a portion of the organic matter can be transformed into bacterial biomass. Culture experiments with mixed substrates show minimal carbon isotopic fractionation during bacterial assimilation (Hullar et al., 1996). However, selective utilization of organic matter by bacteria probably accompanies isotopic fractionation. Macko and Estep (1984) found that bacterial utilization of individual amino acids leads to an increase in bacterial biomass  $\delta^{13}\text{C}$  values (e.g., Alanine,  $+9\text{‰}$ ). Previous research has shown that the  $\delta^{13}\text{C}$  values of amino sugars in heterotrophic bacteria are closely related to their substrates (Guo et al., 2023a). The relatively high  $\delta^{13}\text{C}$  values of amino sugars observed at stations P08 and P09 may be due to the selective assimilation of labile carbon sources, such as amino acids. Guo et al. (2023a) recently proposed the  $V_{\text{AS}}$  index based on the  $\delta^{13}\text{C}$  values of individual amino sugars to assess bacterial re-synthesis. More negative  $V_{\text{AS}}$  value reflects enhanced heterotrophic re-synthesis of amino sugars. In our samples, decreased  $V_{\text{AS}}$  values were observed with increasing salinity (Fig. 8), suggesting active heterotrophic transformation in the

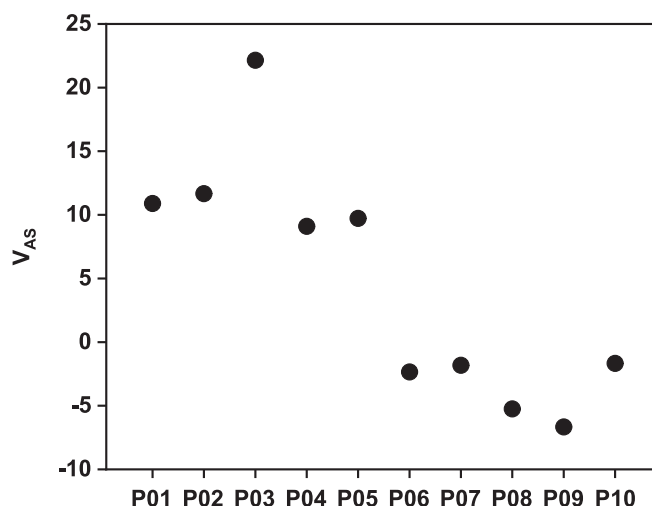


Fig. 8. Index of variation in amino sugar carbon isotopes ( $V_{\text{AS}}$ ) along the Changjiang River-estuary-coastal ocean continuum.  $V_{\text{AS}}$  was calculated based on the differences in  $\delta^{13}\text{C}$  values among individual amino sugars. A more negative  $V_{\text{AS}}$  value indicates enhanced heterotrophic re-synthesis of amino sugars (Guo et al., 2023a).

estuarine area. To further examine the extent of bacterial transformation of POM, we used MurA to quantitatively estimate bacterial POC. Our results show that  $\sim 16\%$  of POC in the Changjiang Estuary and adjacent areas is of bacterial origin, exhibiting a decreasing trend followed by an increase with increasing salinity (Fig. 9). This trend is closely linked to changes in phytoplankton production and the removal of bacterial POC along the salinity gradient. Both autotrophic (in particular, cyanobacteria) and heterotrophic bacteria contribute to bacterial POC based on biomarker determinations. However, in the Changjiang Estuary, cyanobacteria are relatively scarce, particularly in areas with salinities below 20, where their relative abundance is  $< 5\%$  (Jiang et al., 2022). This suggests that the majority of bacterial POC is derived from heterotrophic bacteria. The sharp decline in the proportion of bacterial POC observed in the estuarine region supports the pattern of a rapid decrease in terrestrial organic matter, further highlighting the efficient removal processes occurring within the estuary. We note that the diagenesis of MurA and changes in the bacterial community along the salinity

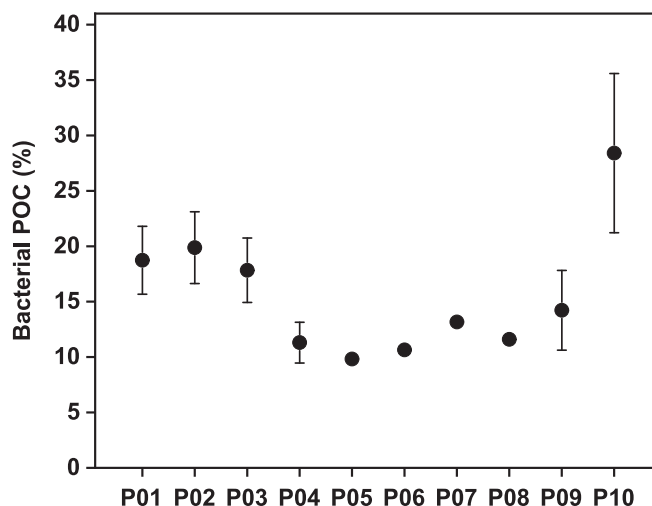


Fig. 9. Bacterial contributions to particulate organic carbon (POC) along the Changjiang River-estuary-coastal ocean continuum. Values were calculated using Eq. (3) and the carbon-normalized yields of muramic acid (MurA). The error bars represent the propagated uncertainties associated with the yields of bacterial MurA.

gradient could bias the bacterial contributions to POC. Particularly, MurA, being a component of peptidoglycan, exhibits higher reactivity relative to bulk bacterial materials (Moriarty, 1977; Nagata et al., 2003; Tremblay and Benner, 2006; Lomstein et al., 2009). It appears to serve as a biomarker for living bacteria and recent bacterial necromass, potentially underestimating the total bacterial contribution (Tremblay and Benner, 2006, 2009; Bourgoïn and Tremblay, 2010). Comparisons of bacterial origins in marine POM based on MurA and cell counts showed that over 2/3 of bacterial organic carbon is represented by bacterial detritus (Khodse and Bhosle, 2013; Ren et al., 2020). These findings suggest that bacterial organic matter inferred from MurA is largely associated with bacterial detritus. Despite these uncertainties with possible influences on the quantitative results, the incubation experiments showed that MurA-based estimates presented consistent trends with bacterial re-synthesis, which was indicated by the decrease in GlcN/GalN (Lehmann et al., 2020).

We observed that ~19% of POC in the Changjiang River comes from bacteria (Fig. 9). Our results reveal an important contribution of bacterial detritus to terrestrial organic matter, which has not been fully appreciated in earlier studies. At the front of the Changjiang River plume, elevated bacterial contributions to POC indicate rapid bacterial transformation. Despite a portion of the bacterial organic matter being involved in rapid cycling, bacterial detritus reactivity is lower than algal organic matter, thus facilitating carbon sequestration. Overall, our results suggest that bacterial organic matter makes a significant contribution to POM in estuarine systems. These findings demonstrate the important role of bacteria in the transformation of organic matter along the river-estuary-coastal ocean continuum.

## 5. Conclusions

This study characterizes the abundance and isotopic composition of POM at both bulk and molecular levels along the river-estuary-coastal ocean continuum. These molecular and compound-specific isotope analyses provide powerful tools for unraveling the complex biogeochemical cycles of organic matter in dynamic estuarine settings. To our knowledge, this study represents the first coupled presentation of  $\delta^{13}\text{C}$  variations in amino sugars and amino acids along the salinity gradient. The main findings are summarized as follows:

- (1) Bulk POC  $\delta^{13}\text{C}$  values reflect the  $\delta^{13}\text{C}$  values of primary producers. The degree of fractionation between phytoplankton  $\delta^{13}\text{C}$  and  $\delta^{13}\text{C}_{\text{DIC}}$  values varies with salinity, with larger offsets occurring in high salinity areas.
- (2) Sources of amino sugars and amino acids are diverse along the salinity gradient. Terrestrial amino acids mainly originate from bacteria and vascular plants, while marine amino acids primarily come from algae. In contrast, amino sugars exhibit a mixed source at the freshwater end, including bacteria, fungi, and algae, transitioning to bacteria towards the sea.
- (3) Terrestrial POM exhibits an advanced diagenetic state, but contributions from phytoplankton production result in elevated POM reactivity in moderate to high salinity zones.
- (4) Bacterial transformation significantly influences the fate of POM. A substantial portion of terrestrial POM originates from bacterial material and undergoes extensive removal in estuarine regions. From the estuary to the coastal ocean, bacterial contributions to POM progressively increase.

These new data provide novel insights into the sources and fate of organic matter in estuarine and coastal areas. Our findings emphasize estuarine regions as crucial organic matter processors, making significant contributions to carbon cycling. Further research is needed to enhance the quantitative applications of amino sugar and amino acid isotopic values in organic matter cycling.

## CRedit authorship contribution statement

**Jinqiang Guo:** Writing – original draft, Methodology, Investigation, Formal analysis, Data curation, Conceptualization. **Eric P. Achterberg:** Writing – review & editing, Resources. **Yuan Shen:** Writing – review & editing, Funding acquisition. **Bu Zhou:** Writing – review & editing, Methodology, Investigation. **Jinming Song:** Writing – review & editing, Supervision, Funding acquisition. **Xuegang Li:** Writing – review & editing. **Liqin Duan:** Writing – review & editing. **Huamao Yuan:** Writing – review & editing, Supervision, Funding acquisition, Data curation.

## Declaration of competing interest

The authors declare that they have no known competing financial interests or personal relationships that could have appeared to influence the work reported in this paper.

## Acknowledgments

We thank the crew of the R/V Runjiang for sampling assistance. This work was supported by the National Natural Science Foundation of China (grant nos. 42276038, 42322602, 42106040), Laoshan Laboratory (grant no. LSKJ202204001), the Shandong Province Natural Science Foundation (grant no. ZR2020YQ28), the Taishan Scholars Program (grant no. tsqn202211256), the Two-Hundred Talents Plan of Yantai Scholar Project Special Funding, the Fundamental Research Funds for the Central Universities of China (grant no. 20720210076), and Fujian Provincial Central Guided Local Science and Technology Development Special Project (grant no. 2022L3078). Jinqiang Guo also thanks the China Scholarship Council (CSC) and Deutscher Akademischer Austauschdienst (DAAD) for additional support.

## References

- Bauer, J.E., Cai, W., Raymond, P.A., Bianchi, T.S., Hopkinson, C.S., Regnier, P.A.G., 2013. The changing carbon cycle of the coastal ocean. *Nature* 504, 61–70.
- Benner, R., Fogel, M.L., Sprague, E.K., Hodson, R.E., 1987. Depletion of  $^{13}\text{C}$  in lignin and its implications for stable carbon isotope studies. *Nature* 329, 708–710.
- Benner, R., Kaiser, K., 2003. Abundance of amino sugars and peptidoglycan in marine particulate and dissolved organic matter. *Limnol. Oceanogr.* 48, 118–128.
- Benner, R., Kaiser, K., 2011. Biological and photochemical transformations of amino acids and lignin phenols in riverine dissolved organic matter. *Biogeochemistry* 102, 209–222.
- Bianchi, T.S., 2007. *Biogeochemistry of Estuaries*. Oxford University Press, Oxford.
- Bianchi, T.S., 2011. The role of terrestrially derived organic carbon in the coastal ocean: A changing paradigm and the priming effect. *P. Natl. Acad. Sci. USA* 108, 19473–19481.
- Bianchi, T.S., Canuel, E.A., 2011. *Chemical Biomarkers in Aquatic Ecosystems*. Princeton University Press, Princeton.
- Bianchi, T.S., Mayer, L.M., Amaral, J.H.F., Arndt, S., Galy, V., Kemp, D.B., Kuehl, S.A., Murray, N.J., Regnier, P., 2024. Anthropogenic impacts on mud and organic carbon cycling. *Nat. Geosci.* 17, 287–297.
- Bianchi, T.S., Thornton, D.C.O., Yvon-Lewis, S.A., King, G.M., Eglinton, T.I., Shields, M. R., Ward, N.D., Curtis, J., 2015. Positive priming of terrestrially derived dissolved organic matter in a freshwater microcosm system. *Geophys. Res. Lett.* 42, 5460–5467.
- Blair, N.E., Aller, R.C., 2012. The fate of terrestrial organic carbon in the marine environment. *Annu. Rev. Mar. Sci.* 4, 401–423.
- Bodé, S., Deneff, K., Boeckx, P., 2009. Development and evaluation of a high-performance liquid chromatography/isotope ratio mass spectrometry methodology for  $\delta^{13}\text{C}$  analyses of amino sugars in soil. *Rapid Commun. Mass Sp.* 23, 2519–2526.
- Bourgoïn, L.H., Tremblay, L., 2010. Bacterial reworking of terrigenous and marine organic matter in estuarine water columns and sediments. *Geochim. Cosmochim. Acta* 74, 5593–5609.
- Brutemark, A., Lindehoff, E., Granéli, E., Granéli, W., 2009. Carbon isotope signature variability among cultured microalgae: Influence of species, nutrients and growth. *J. Exp. Mar. Biol. Ecol.* 372, 98–105.
- Burkhardt, S., Riebesell, U., Zondervan, I., 1999. Stable carbon isotope fractionation by marine phytoplankton in response to daylength, growth rate, and  $\text{CO}_2$  availability. *Mar. Ecol. Prog. Ser.* 184, 31–41.
- Cai, W., 2011. Estuarine and coastal ocean carbon paradox:  $\text{CO}_2$  sinks or sites of terrestrial carbon incineration? *Annu. Rev. Mar. Sci.* 3, 123–145.
- Canuel, E.A., Hardison, A.K., 2016. Sources, ages, and alteration of organic matter in estuaries. *Annu. Rev. Mar. Sci.* 8, 409–434.

- Chanton, J.P., Lewis, F.G., 1999. Plankton and dissolved inorganic carbon isotopic composition in a river-dominated estuary: Apalachicola Bay, Florida. *Estuar. 22*, 575–583.
- Chen, H., Abdulla, H.A.N., Sanders, R.L., Myneni, S.C.B., Mopper, K., Hatcher, P.G., 2014. Production of black carbon-like and aliphatic molecules from terrestrial dissolved organic matter in the presence of sunlight and iron. *Environ. Sci. Technol. Lett. 1*, 399–404.
- Cloern, J.E., Canuel, E.A., Harris, D., 2002. Stable carbon and nitrogen isotope composition of aquatic and terrestrial plants of the San Francisco Bay estuarine system. *Limnol. Oceanogr. 47*, 713–729.
- Cloern, J.E., Foster, S.Q., Kleckner, A.E., 2014. Phytoplankton primary production in the world's estuarine-coastal ecosystems. *Biogeosciences 11*, 2477–2501.
- Cowie, G.L., Hedges, J.L., 1994. Biochemical indicators of diagenetic alteration in natural organic matter mixtures. *Nature 369*, 304–307.
- Dagg, M., Benner, R., Lohrenz, S., Lawrence, D., 2004. Transformation of dissolved and particulate materials on continental shelves influenced by large rivers: plume processes. *Cont. Shelf Res. 24*, 833–858.
- Dai, M., Cao, Z., Guo, X., Zhai, W., Liu, Z., Yin, Z., Xu, Y., Gan, J., Hu, J., Du, C., 2013. Why are some marginal seas sources of atmospheric CO<sub>2</sub>? *Geophys. Res. Lett. 40*, 2154–2158.
- Dai, M., Su, J., Zhao, Y., Hofmann, E.E., Cao, Z., Cai, W.J., Gan, J., Lacroix, F., Laruelle, G.G., Meng, F., Mueller, J.D., Regnier, P.A.G., Wang, G., Wang, Z., 2022. Carbon fluxes in the coastal ocean: Synthesis, boundary processes, and future trends. *Annu. Rev. Earth Pl. Sc. 50*, 593–626.
- Dauwe, B., Middelburg, J., Herman, P., Heip, C., 1999. Linking diagenetic alteration of amino acids and bulk organic matter reactivity. *Limnol. Oceanogr. 44*, 1809–1814.
- Davis, J., Kaiser, K., Benner, R., 2009. Amino acid and amino sugar yields and compositions as indicators of dissolved organic matter diagenesis. *Org. Geochem. 40*, 343–352.
- Erez, J., Bouevitch, A., Kaplan, A., 1998. Carbon isotope fractionation by photosynthetic aquatic microorganisms: experiments with *Synechococcus* PCC7942, and a simple carbon flux model. *Can. J. Bot. 76*, 1109–1118.
- Feng, X., Hills, K.M., Simpson, A.J., Whalen, J.K., Simpson, M.J., 2011. The role of biodegradation and photo-oxidation in the transformation of terrigenous organic matter. *Org. Geochem. 42*, 262–274.
- Fichot, C.G., Benner, R., 2014. The fate of terrigenous dissolved organic carbon in a river-influenced ocean margin. *Global Biogeochem. Cy. 28*, 300–318.
- Gattuso, J., Frankignoulle, M., Wollast, R., 1998. Carbon and carbonate metabolism in coastal aquatic ecosystems. *Annu. Rev. Ecol. Evol. S. 29*, 405–434.
- Guo, J., Achterberg, E.P., Shen, Y., Yuan, H., Song, J., Liu, J., Li, X., Duan, L., 2023a. Stable carbon isotopic composition of amino sugars in heterotrophic bacteria and phytoplankton: Implications for assessment of marine organic matter degradation. *Limnol. Oceanogr. 68*, 2814–2825.
- Guo, J., Liang, S., Wang, X., Pan, X., 2021a. Distribution and dynamics of dissolved organic matter in the Changjiang Estuary and adjacent sea. *J. Geophys. Res-Bioge. 126*, e2020JG006161.
- Guo, J., Shen, Y., Yuan, H., Song, J., Li, X., Duan, L., Li, N., 2023b. Bacterial reworking of particulate organic matter in a dynamic marginal sea: Implications for carbon sequestration. *Org. Geochem. 179*, 104583.
- Guo, J., Yuan, H., Song, J., Li, X., Duan, L., Li, N., Wang, Y., 2021b. Evaluation of sedimentary organic carbon reactivity and burial in the eastern China marginal seas. *J. Geophys. Res-Oceans 126*, e2021JC017207.
- Guo, W., Ye, F., Xu, S., Jia, G., 2015. Seasonal variation in sources and processing of particulate organic carbon in the Pearl River estuary. *South China. Estuar. Coast. Shelf S. 167*, 540–548.
- Hedges, J.L., Keil, R.G., Benner, R., 1997. What happens to terrestrial organic matter in the ocean? *Org. Geochem. 27*, 195–212.
- Helms, J.R., Mao, J., Schmidt-Rohr, K., Abdulla, H., Mopper, K., 2013. Photochemical flocculation of terrestrial dissolved organic matter and iron. *Geochim. Cosmochim. Acta 121*, 398–413.
- Hinga, K.R., Arthur, M.A., Pilson, M.E.Q., Whitaker, D., 1994. Carbon isotope fractionation by marine phytoplankton in culture: The effects of CO<sub>2</sub> concentration, pH, temperature, and species. *Global Biogeochem. Cy. 8*, 91–102.
- Howland, M.R., Corr, L.T., Young, S.M.M., Jones, V., Jim, S., Van Der Merwe, N.J., Mitchell, A.D., Evershed, R.P., 2003. Expression of the dietary isotope signal in the compound-specific  $\delta^{13}\text{C}$  values of pig bone lipids and amino acids. *Int. J. Osteoarchaeol. 13*, 54–65.
- Hullar, M., Fry, B., Peterson, B., Wright, R., 1996. Microbial utilization of estuarine dissolved organic carbon: a stable isotope tracer approach tested by mass balance. *Appl. Environ. Microbiol. 62*, 2489–2493.
- Jiang, X., Lu, B., He, Y., 2013. Response of the turbidity maximum zone to fluctuations in sediment discharge from river to estuary in the Changjiang Estuary (China). *Estuar. Coast. Shelf S. 131*, 24–30.
- Jiang, X., Zhu, Z., Wu, J., Lian, E., Liu, D., Yang, S., Zhang, R., 2022. Bacterial and protistan community variation across the Changjiang Estuary to the ocean with multiple environmental gradients. *Microorganisms 10*, 991.
- Jiang, Z., Chen, J., Zhou, F., Shou, L., Chen, Q., Tao, B., Yan, X., Wang, K., 2015. Controlling factors of summer phytoplankton community in the Changjiang (Yangtze River) Estuary and adjacent East China Sea shelf. *Cont. Shelf Res. 101*, 71–84.
- Joergensen, R.G., 2018. Amino sugars as specific indices for fungal and bacterial residues in soil. *Biol. Fert. Soils 54*, 559–568.
- Kaiser, K., Benner, R., 2000. Determination of amino sugars in environmental samples with high salt content by high-performance anion-exchange chromatography and pulsed amperometric detection. *Anal. Chem. 72*, 2566–2572.
- Kaiser, K., Benner, R., 2008. Major bacterial contribution to the ocean reservoir of detrital organic carbon and nitrogen. *Limnol. Oceanogr. 53*, 99–112.
- Kang, P., Zhang, H., Yang, Z., Zhu, Y., He, B., Li, Q., Lee, C., Tang, T., 2021. A model of algal organic carbon distributions in the Pearl River estuary using the amino acid carbon isotope values. *Geochim. Cosmochim. Acta 294*, 1–12.
- Khodse, V.B., Bhosle, N.B., 2013. Distribution, origin and transformation of amino sugars and bacterial contribution to estuarine particulate organic matter. *Cont. Shelf Res. 68*, 33–42.
- Lamb, A.L., Wilson, G.P., Leng, M.J., 2006. A review of coastal palaeoclimate and relative sea-level reconstructions using  $\delta^{13}\text{C}$  and C/N ratios in organic material. *Earth-Sci. Rev. 75*, 29–57.
- Larsen, T., Ventura, M., Andersen, N., O'Brien, D.M., Piatkowski, U., McCarthy, M.D., 2013. Tracing carbon sources through aquatic and terrestrial food webs using amino acid stable isotope fingerprinting. *PLoS One 8*, e73441.
- Leboulanger, C., Descolas-Gros, C., Fontugne, M.R., Bentele, I., Jupin, H., 1995. Interspecific variability and environmental influence on particulate organic carbon  $\delta^{13}\text{C}$  in cultured marine phytoplankton. *J. Plankton Res. 17*, 2079–2091.
- Lehmann, M.F., Carstens, D., Deek, A., McCarthy, M., Schubert, C.J., Zoppi, J., 2020. Amino acid and amino sugar compositional changes during in vitro degradation of algal organic matter indicate rapid bacterial re-synthesis. *Geochim. Cosmochim. Acta 283*, 67–84.
- Li, H., Tang, H., Shi, X., Zhang, C., Wang, X., 2014. Increased nutrient loads from the Changjiang (Yangtze) River have led to increased harmful algal blooms. *Harmful Algae 39*, 92–101.
- Liang, S., Li, S., Guo, J., Yang, Y., Xu, Z., Zhang, M., Li, H., Yu, X., Ma, H., Wang, X., 2023. Source, composition, and reactivity of particulate organic matter along the Changjiang Estuary salinity gradient and adjacent sea. *Mar. Chem. 252*.
- Lindroth, P., Mopper, K., 1979. High performance liquid chromatographic determination of subpicomole amounts of amino acids by precolumn fluorescence derivatization with o-phthalaldehyde. *Anal. Chem. 51*, 1667–1674.
- Lomstein, B.A., Niggemann, J., Jørgensen, B.B., Langerhuusa, A.T., 2009. Accumulation of prokaryotic remains during organic matter diagenesis in surface sediments off Peru. *Limnol. Oceanogr. 54*, 1139–1151.
- Macko, S.A., Estep, M.L.F., 1984. Microbial alteration of stable nitrogen and carbon isotopic compositions of organic matter. *Org. Geochem. 6*, 787–790.
- McCallister, S.L., Bauer, J.E., Kelly, J., Ducklow, H.W., 2005. Effects of sunlight on decomposition of estuarine dissolved organic C, N and P and bacterial metabolism. *Aquat. Microb. Ecol. 40*, 25–35.
- McCarthy, M.D., Lehman, J., Kudela, R., 2013. Compound-specific amino acid  $\delta^{15}\text{N}$  patterns in marine algae: Tracer potential for cyanobacterial vs. eukaryotic organic nitrogen sources in the ocean. *Geochim. Cosmochim. Acta 103*, 104–120.
- McMahon, K.W., Fogel, M.L., Elsdon, T.S., Thorrold, S.R., 2010. Carbon isotope fractionation of amino acids in fish muscle reflects biosynthesis and isotopic routing from dietary protein. *J. Anim. Ecol. 79*, 1132–1141.
- McMahon, K.W., Williams, B., Guilderson, T.P., Glynn, D.S., McCarthy, M.D., 2018. Calibrating amino acid  $\delta^{13}\text{C}$  and  $\delta^{15}\text{N}$  offsets between polyp and protein skeleton to develop proteinaceous deep-sea corals as paleoceanographic archives. *Geochim. Cosmochim. Acta 220*, 261–275.
- Middelburg, J.J., Herman, P.M.J., 2007. Organic matter processing in tidal estuaries. *Mar. Chem. 106*, 127–147.
- Moriarty, D.J.W., 1977. Improved method using muramic acid to estimate biomass of bacteria in sediments. *Oecologia 26*, 317–323.
- Müller, P.J., Suess, E., Ungerer, C.A., 1986. Amino acids and amino sugars of surface particulate and sediment trap material from waters of the Scotia Sea. *Deep Sea Res. A 33*, 819–838.
- Nagata, T., Meon, B.L., Kirchman, D., 2003. Microbial degradation of peptidoglycan in seawater. *Limnol. Oceanogr. 48*, 745–754.
- Opsahl, S., Benner, R., 1998. Photochemical reactivity of dissolved lignin in river and ocean waters. *Limnol. Oceanogr. 43*, 1297–1304.
- Opsahl, S.P., Zepp, R.G., 2001. Photochemically-induced alteration of stable carbon isotope ratios ( $\delta^{13}\text{C}$ ) in terrigenous dissolved organic carbon. *Geophys. Res. Lett. 28*, 2417–2420.
- Parsons, J.W., 2021. Chemistry and distribution of amino sugars in soils and soil organisms. In: Paul, E.A., Ladd, J.N. (Eds.), *Soil Biochemistry*. CRC Press, Boca Raton, pp. 197–228.
- Popp, B.N., Laws, E.A., Bidigare, R.R., Dore, J.E., Hanson, K.L., Wakeham, S.G., 1998. Effect of phytoplankton cell geometry on carbon isotopic fractionation. *Geochim. Cosmochim. Acta 62*, 69–77.
- Ren, C., Yuan, H., Song, J., Duan, L., Li, X., Li, N., Zhou, B., 2020. The use of amino sugars for assessing seasonal dynamics of particulate organic matter in the Yangtze River estuary. *Mar. Chem. 220*.
- Sanches, L.F., Guenet, B., Marino, N.A.C., de Assis Esteves, F., 2021. Exploring the drivers controlling the priming effect and its magnitude in aquatic systems. *J. Geophys. Res-Bioge. 126*, e2020JG006201.
- Shen, Y., Benner, R., Murray, A.E., Gimpel, C., Mitchell, B.G., Weiss, E.L., Reiss, C., 2017. Bioavailable dissolved organic matter and biological hot spots during austral winter in Antarctic waters. *J. Geophys. Res-Oceans 122*, 508–520.
- Silfer, J.A., Engel, M.H., Macko, S.A., Jumeau, E.J., 1991. Stable carbon isotope analysis of amino acid enantiomers by conventional isotope ratio mass spectrometry and combined gas chromatography/isotope ratio mass spectrometry. *Anal. Chem. 63*, 370–374.
- Snedden, G.A., Cable, J.E., Kjerfve, B., 2013. Estuarine geomorphology and coastal hydrology. In: John, W.D., Byron, C.C., W. Michael, K., Alejandro, Y.A. (Eds.), *Estuarine Ecology*. John Wiley & Sons Inc., Hoboken, pp. 19–38.
- Stubbins, A., Spencer, R.G.M., Chen, H., Hatcher, P.G., Mopper, K., Hernes, P.J., Mwamba, V.L., Mangangu, A.M., Wabakanghanzi, J.N., Six, J., 2010. Illuminated darkness: Molecular signatures of Congo River dissolved organic matter and its

- photochemical alteration as revealed by ultrahigh precision mass spectrometry. *Limnol. Oceanogr.* 55, 1467–1477.
- Tremblay, L., Benner, R., 2006. Microbial contributions to N-immobilization and organic matter preservation in decaying plant detritus. *Geochim. Cosmochim. Acta* 70, 133–146.
- Tremblay, L., Benner, R., 2009. Organic matter diagenesis and bacterial contributions to detrital carbon and nitrogen in the Amazon River system. *Limnol. Oceanogr.* 54, 681–691.
- Waggoner, D.C., Chen, H., Willoughby, A.S., Hatcher, P.G., 2015. Formation of black carbon-like and alicyclic aliphatic compounds by hydroxyl radical initiated degradation of lignin. *Org. Geochem.* 82, 69–76.
- Waggoner, D.C., Hatcher, P.G., 2017. Hydroxyl radical alteration of HPLC fractionated lignin: Formation of new compounds from terrestrial organic matter. *Org. Geochem.* 113, 315–325.
- Wang, X., Luo, C., Ge, T., Xu, C., Xue, Y., 2016. Controls on the sources and cycling of dissolved inorganic carbon in the Changjiang and Huanghe River estuaries, China:  $^{14}\text{C}$  and  $^{13}\text{C}$  studies. *Limnol. Oceanogr.* 61, 1358–1374.
- Wang, Y., Wu, H., Gao, L., Shen, F., Liang, X.S., 2019. Spatial distribution and physical controls of the spring algal blooming off the Changjiang River Estuary. *Estuar. Coast.* 42, 1066–1083.
- Welschmeyer, N.A., 1994. Fluorometric analysis of chlorophyll a in the presence of chlorophyll b and pheopigments. *Limnol. Oceanogr.* 39, 1985–1992.
- Wu, Y., Dittmar, T., Ludwigowski, K., Kattner, G., Zhang, J., Zhu, Z., Koch, B., 2007. Tracing suspended organic nitrogen from the Yangtze River catchment into the East China Sea. *Mar. Chem.* 107, 367–377.
- Xing, L., Zhang, H., Yuan, Z., Sun, Y., Zhao, M., 2011. Terrestrial and marine biomarker estimates of organic matter sources and distributions in surface sediments from the East China Sea shelf. *Cont. Shelf Res.* 31, 1106–1115.
- Xu, M.N., Zhang, W., Zhu, Y., Liu, L., Zheng, Z., Wan, X.S., Qian, W., Dai, M., Gan, J., Hutchins, D.A., Kao, S.J., 2018. Enhanced ammonia oxidation caused by lateral Kuroshio intrusion in the boundary zone of the northern South China Sea. *Geophys. Res. Lett.* 45, 6585–6593.
- Yao, P., Yu, Z., Bianchi, T.S., Guo, Z., Zhao, M., Knappy, C.S., Keely, B.J., Zhao, B., Zhang, T., Pan, H., Wang, J., Li, D., 2015. A multiproxy analysis of sedimentary organic carbon in the Changjiang Estuary and adjacent shelf. *J. Geophys. Res.-Biogeo.* 120, 1407–1429.
- Yao, W., Dong, Y., Qi, Y., Han, Y., Ge, J., Volmer, D.A., Zhang, Z., Liu, X., Li, S.L., Fu, P., 2025. Tracking the changes of DOM composition, transformation, and cycling mechanism triggered by the priming effect: Insights from incubation experiments. *Environ. Sci. Technol.* 59, 430–442.
- Yin, G., Zhang, P., Wang, Y., Aftab, B., Du, P., Zhang, Q., Chen, G., Wang, M., Yang, B., Wang, S., Mo, J., Zhang, W., Wang, J., 2023. Photochemical transformation of terrestrial dissolved organic matter derived from multiple sources in tropical plantations. *Geochim. Cosmochim. Acta* 358, 162–173.
- Zhai, W., Dai, M., Guo, X., 2007. Carbonate system and  $\text{CO}_2$  degassing fluxes in the inner estuary of Changjiang (Yangtze) River. *China. Mar. Chem.* 107, 342–356.
- Zhu, R., Lin, Y.S., Lipp, J.S., Meador, T.B., Hinrichs, K.U., 2014. Optimizing sample pretreatment for compound-specific stable carbon isotopic analysis of amino sugars in marine sediment. *Biogeosciences* 11, 4869–4880.
- Zhu, Z., Zhang, J., Wu, Y., Lin, J., 2006. Bulk particulate organic carbon in the East China Sea: Tidal influence and bottom transport. *Prog. Oceanogr.* 69, 37–60.
- Zhu, Z., Zhang, J., Wu, Y., Zhang, Y., Lin, J., Liu, S., 2011. Hypoxia off the Changjiang (Yangtze River) Estuary: Oxygen depletion and organic matter decomposition. *Mar. Chem.* 125, 108–116.